ISSN 1560-3547, Regular and Chaotic Dynamics © Pleiades Publishing, Ltd.

Dynamics and Geometry Near Resonant Bifurcations

Henk W. Broer[1*], Sijbo J. Holtman[1], Gert Vegter[1***], and Renato Vitolo[2****]**

[1] *Johann Bernoulli Institute for Mathematics and Computer Science*
University of Groningen, P.O. Box 407, 9700 AK Groningen, The Netherlands

[2] *College of Engineering, Mathematics and Physical Sciences,*
University of Exeter, North Park Road, Exeter EX4 4QF, UK

Received April 04, 2010; accepted June 21, 2010

Abstract This paper provides an overview of the universal study of families of dynamical systems undergoing a Hopf–Neĭmarck–Sacker bifurcation as developed in [1–4]. The focus is on the local resonance set, i.e., regions in parameter space for which periodic dynamics occurs. A classification of the corresponding geometry is obtained by applying Poincaré–Takens reduction, Lyapunov–Schmidt reduction and contact-equivalence singularity theory, equivariant under an appropriate cyclic group. It is a classical result that the local geometry of these sets in the non-degenerate case is given by an Arnol'd resonance tongue. In a mildly degenerate situation a more complicated geometry given by a singular perturbation of a Whitney umbrella is encountered. Our approach also provides a skeleton for the local resonant Hopf–Neĭmarck–Sacker dynamics in the form of planar Poincaré–Takens vector fields. To illustrate our methods a leading example is used: A periodically forced generalized Duffing–Van der Pol oscillator.

MSC2010 numbers: 37G15, 37G40, 34C25, 34C29

DOI: 10.1134/S1560354710520023

Key words: Periodically forced oscillator, Resonant Hopf-Neimarck-Sacker bifurcation, Geometric structure, Lyapunov-Schmidt reduction, Equivariant singularity theory

1. INTRODUCTION

This paper reviews the study of resonant Hopf–Neĭmarck–Sacker (HNS) bifurcations in families of continuous and discrete dynamical systems as presented in [1–4]. The main topic is a novel procedure to detect such bifurcations for the well-known non-degenerate and a mildly degenerate situation. Especially the investigation of the mildly degenerate resonant HNS bifurcation goes beyond known results, since it corresponds to a next case in the general program for recognizing bifurcations, cf. [5, 6]. Moreover, by considering Poincaré–Takens normal form vector field families we show that given the degeneracy the local bifurcation diagram is approximately known.

Leading example. Continuous systems that typically give rise to resonant HNS bifurcations are given by, e.g., coupled oscillators, cell-networks, high dimensional autonomous systems, and periodically forced oscillators. To fix thoughts we consider an example of the latter type: A periodically forced generalized Duffing–Van der Pol oscillator [7, 8] given by

$$\ddot{u} + (\nu_1 + \nu_3 u^2)\dot{u} + \nu_2 u + \nu_4 u^3 + u^5 = \varepsilon(1 + u^6)\cos(2\pi t), \tag{1.1}$$

where $u \in \mathbb{R}$, $t \in \mathbb{R}$, ε is a small positive real constant and $\nu = (\nu_1, \nu_2, \nu_3, \nu_4) \in \mathbb{R}^4$ is a multi-parameter. We note that a necessary requirement for (1.1) to exhibit resonance is that $\nu_1 < 0$ and $\nu_2 > 0$. Furthermore, including the terms of degree 5 and 6 in u turns out to be one of the simplest generalizations of the standard Duffing–Van der Pol oscillator ensuring that (1.1) does not exhibit

*E-mail: H.W.Broer@rug.nl
**E-mail: S.J.Holtman@rug.nl
***E-mail: G.Vegter@rug.nl
****E-mail: R.Vitolo@exeter.ac.uk

too degenerate resonance phenomena. Both Duffing and Van der Pol type oscillators originate from electrical circuits [9, 10].

Resonance. We speak of resonance when a dynamical system contains interacting oscillatory subsystems with rationally related frequencies. To obtain an appropriate form for investigating resonant dynamics in the Duffing–Van der Pol family, we rewrite (1.1) in system form,

$$\begin{aligned} \dot{u} &= v, \\ \dot{v} &= -(\nu_1 + \nu_3 u^2)v - \nu_2 u - \nu_4 u^3 - u^5 + \varepsilon(1+u^6)\cos(2\pi t), \\ \dot{t} &= 1, \end{aligned} \tag{1.2}$$

where $(u, v, t) \in \mathbb{R}^2 \times \mathbb{R}/\mathbb{Z}$. For $\varepsilon = 0$ and without the t-component the system has an equilibrium at $(u, v) = (0, 0)$. Since t runs over a circle, including the t-component causes this equilibrium to become a periodic evolution of (1.2) that goes through $(u, v, t) = (0, 0, 0)$, see Fig. 1. To study the dynamics near this periodic evolution we focus on a section of state space with a constant t-value and on the corresponding discrete dynamics induced by the period-1-map, or Poincaré map, P of the "ow of (1.2). The periodic evolution of (1.2) leads to a fixed point of P , which for small positive values of ε is given by $(u, v) = (0, 0) + O(\varepsilon)$. Since system (1.1) consists of two oscillatory subsystems, given by the periodic forcing and the Duffing–Van der Pol oscillator, we expect that resonant dynamics occurs for certain ν-values. For P this phenomenon shows itself as q-periodic orbits near the fixed point, see Fig. 1. The evolution of (1.2) that gives rise to such periodic orbits are called subharmonics of order q. As the q-periodic orbits are typically situated on an invariant circle, the corresponding subharmonics close after going p times around in a direction transversal to the t-direction and q times around in the t-direction on an invariant torus. In this case we speak of $p : q$-resonance.

We are especially interested in resonance sets, i.e., regions in parameter space for which q-periodic orbits of the Poincaré map occur. On the boundary of these sets the number of these orbits typically changes through a saddle-node bifurcation. Depending on the degeneracy several geometries are possible for the resonance set.

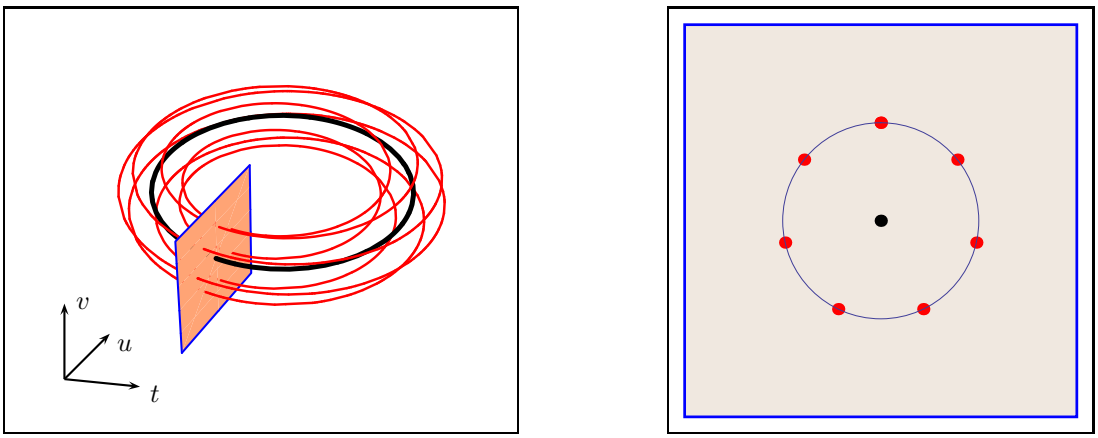

Fig. 1. Left: Sketch of (u, v, t) state space showing a section with t constant, a periodic evolution (thick curve) and a subharmonic of order 7 (thin curve). Right: Sketch of the section with t constant in the left panel, indicating a fixed point and a 7-periodic orbit of the Poincaré map P on an invariant circle.

1.1. Classical Non-degenerate Resonance

Our approach recovers that the simplest resonance scenario is given by the weakly resonant ($q \geqslant 5$) non-degenerate case. In this situation the resonance set is formed by a well-known tongue shaped region, the so-called Arnol'd resonance tongue [5]. Upon passage of the corresponding boundaries a pair of subharmonics appears or merges in state space, see Fig. 2. The tip of the tongue

is called a resonant Hopf–Neĭmarck–Sacker (HNS) bifurcation point, since at this parameter value the resonance set is attached to a set of Hopf–Neĭmarck–Sacker (HNS) bifurcations. If the latter set of bifurcations is crossed transversally in parameter space, then a fixed point of the Poincaré map undergoes a change in stability causing an invariant circle to branch off or merge with the fixed point, again see Fig. 2.

Recognition problem. One of our main aims is to solve the recognition problem for $p:q$-resonant HNS bifurcations, i.e., provide conditions that determine the parameter values for which such a bifurcation occurs. A first condition these parameter values should satisfy is that the linear part of the Poincaré map at a fixed point has a pair of eigenvalues of the form $e^{\pm 2\pi i p/q}$ with $0 < |p| < q \in \mathbb{N}$ and $\gcd(p,q) = 1$. Secondly, the degeneracy of the bifurcation depends on higher order derivatives at the central bifurcation point. In [3] an explicit set of polynomial conditions in finite order coefficients of the series expansion of a periodically forced oscillator is presented that determine which parameter values correspond to a non-degenerate resonant HNS bifurcation. For example, for the system given in (1.2), with $(p,q) = (1,7)$, we obtain that the tip of the Arnol'd tongue is located on the following 2-dimensional subset of parameter space:

$$\left\{\nu \in \mathbb{R}^4 \mid \nu_1 = 0, \nu_2 = \tfrac{4}{49}\pi^2, \nu_3^2 + \nu_4^2 \neq 0\right\}. \tag{1.3}$$

The equalities $\nu_1 = 0$ and $\nu_2 = \frac{4}{49}\pi^2$ ensure that the critical eigenvalues of the Jacobian of the Poincaré map at the central fixed point are of the form $e^{\pm 2\pi i/7}$ and the inequality $\nu_3^2 + \nu_4^2 \neq 0$ causes appropriate higher order coefficients in a series expansion of (1.2) to be non-zero. We note that all these conditions are computed up to order $O(\varepsilon)$.

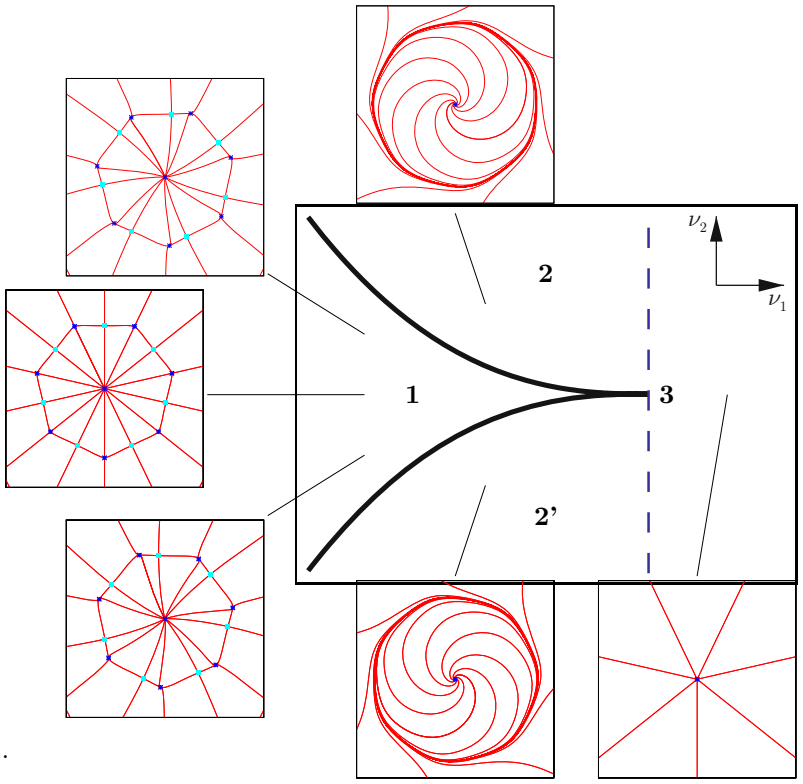

Fig. 2. Sketch of the bifurcation diagram of a Poincaré map of the forced Duffing–Van der Pol system given in (1.2) for $q = 7$ and fixed non-zero values of ν_3, ν_4 and ε. The bifurcation set, a subset of parameter space given by parameter values for which there is a qualitative change in the dynamics, consists of the cusp-shaped boundary of an Arnol'd resonance tongue and a dashed Hopf–Neĭmarck–Sacker (HNS) line. The phase portraits show that for region 1 there are two 7-periodic orbits of the Poincaré map on an invariant circle that merge at the boundary. Moreover, the invariant circle merges with the central fixed point if the HNS-line is crossed from left to right.

Central questions. The dynamics of the forced Duffing–Van der Pol system described above occurs in all generic 2-parameter families of smooth (Poincaré) maps undergoing a non-degenerate resonant HNS bifurcation. This is a classical result, so we are more interested in a next case corresponding to mildly degenerate weakly resonant ($q \geqslant 7$) HNS bifurcations. This situation is encountered in generic 4-parameter families. To be more precise, the main part of the current work deals with the following central questions:

1. How to detect, or recognize, a mildly degenerate resonant HNS bifurcation in a given family of smooth (Poincaré) maps?

2. What is the generic local geometry of the resonance set attached to a mildly degenerate resonant HNS bifurcation?

3. What is the generic local bifurcation diagram near a mildly degenerate resonant HNS bifurcation?

We note that the resonance set only gives information on bifurcations of q-periodic orbits of maps, while the bifurcation set also incorporates other types of bifurcations involving, e.g., invariant circles and stable and unstable manifolds.

To solve the first two central questions we apply Lyapunov–Schmidt reduction, which maps a family of maps near $p:q$-resonance to a family of $\mathbb{Z}_q$-equivariant maps, such that the zeros of the latter family correspond to periodic orbits of the former family. Then $\mathbb{Z}_q$-equivariant contact-equivalence singularity theory is utilized to obtain recognition conditions and the geometry of the resonance set for the mildly degenerate case. To answer the third central question we apply the Poincaré–Takens normal form procedure, which provides an approximating family of vector fields for the family of (Poincaré) maps. The dynamics of the latter family is investigated by studying the vector field family using (numerical) methods from bifurcation theory.

1.2. Mildly Degenerate Resonance

We continue discussing mildly degenerate resonant HNS bifurcations in the Duffing–Van der Pol family given in (1.2). In particular, we focus on a $1:7$-resonance, since this is the strongest mildly degenerate weak resonance. We note that the geometry and dynamics described here is generic and, therefore, occurs in all families of smooth (Poincaré) maps undergoing a mildly degenerate HNS bifurcation.

Recognition problem. We start with the solution of the recognition problem. By using the tools presented in [3], which amounts to checking a set of polynomial conditions in finite order coefficients of a series expansion of (1.2), we arrive at the following result. System (1.1) undergoes a mildly degenerate $1:7$-resonant HNS bifurcation for the following 0-dimensional subset of parameter space:

$$\left\{\nu \in \mathbb{R}^4 \mid \nu_1 = 0, \nu_2 = \tfrac{4}{49}\pi^2, \nu_3 = 0, \nu_4 = 0\right\}. \tag{1.4}$$

This set is computed up to order $O(\varepsilon)$. The difference with the recognition conditions for the non-degenerate case given in (1.3) is that here both ν_3 and ν_4 are equal to 0.

The boundary of the resonance set attached to the parameter value given in (1.4) is diffeomorphic to the discriminant set of a 4-parameter normal form family, see the next section. To display the geometry of this set we take 2-dimensional cross-sections of parameter space, see Fig. 3, which indicates the presence of cusps and a swallowtail. The normal form family also provides a skeleton for the local dynamics. To understand this we first explain the Poincaré–Takens normal form procedure.

Poincaré Takens normal form. The Duffing–Van der Pol system given in (1.2) is of the appropriate form to apply Poincaré–Takens reduction. In fact, every system of the form

$$\begin{aligned} \dot{y} &= h_\mu(y) + \varepsilon H_\mu(y,t), \\ \dot{t} &= 1 \end{aligned} \tag{1.5}$$

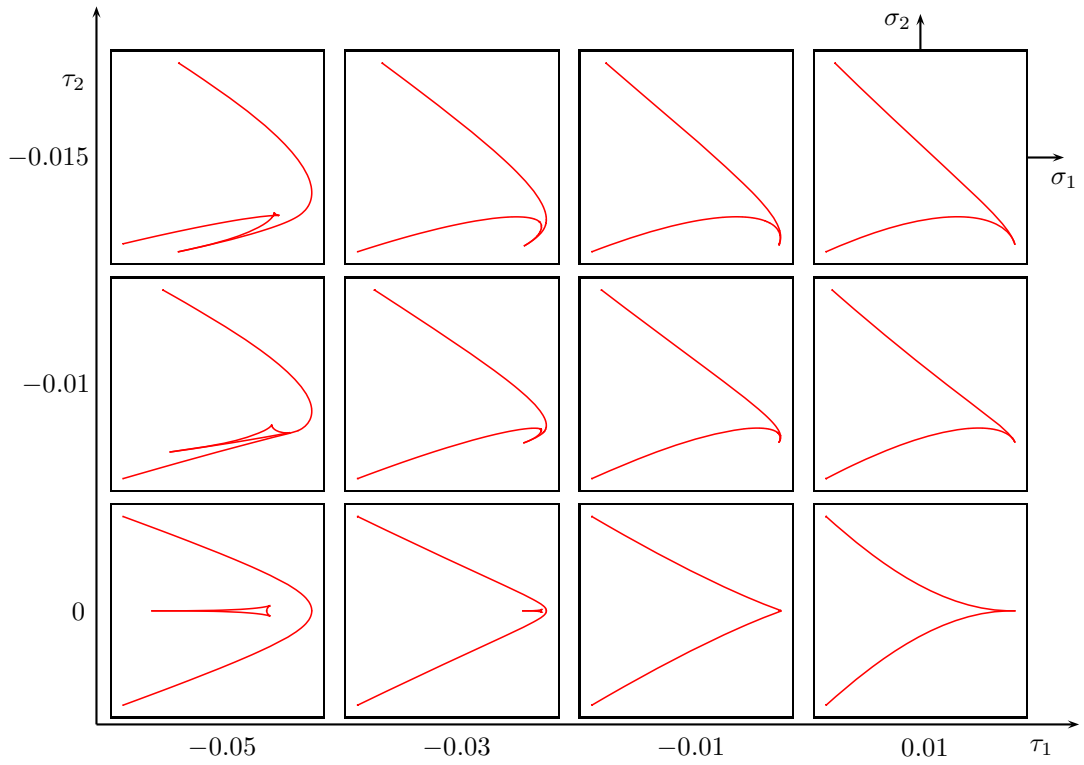

Fig. 3. The generic geometry of the boundary of the resonance set in the mildly degenerate case for $q = 7$ is depicted in several 2-dimensional cross-sections of 4-dimensional parameter space. To be precise, the displayed boundary is obtained as the discriminant set of the 4-parameter normal form $\mathcal{G}_{\sigma,\tau}$, with $(\sigma, \tau) = (\sigma_1 + i\sigma_2, \tau_1 + i\tau_2)$, given later on in (1.8). Because of a symmetry of $\mathcal{G}_{\sigma,\tau}$, only cross-sections for positive τ_2-values are given. Moreover, only one positive τ_1-value is considered, since for all small positive τ_1-values the boundary of the resonance set is cusp-shaped. The top left panel indicates the presence of a swallowtail-geometry. Concerning the number of periodic orbits, we have that for parameter values inside the displayed triangular regions four local 7-periodic orbits exist of which two merge on the corresponding boundary. If next also the outer boundary is crossed in parameter space, then the remaining pair of local 7-periodic orbits merges.

fits the current framework. We note that h_μ and H_μ depend smoothly on both the multi-parameter $\mu = (\mu_1, \ldots, \mu_n) \in \mathbb{R}^n$ and the coordinates $y \in \mathbb{C}$ or $(y, t) \in \mathbb{C} \times \mathbb{R}/\mathbb{Z}$, respectively (for convenience we identify $\mathbb{R}^2$ with $\mathbb{C}$). Moreover, we assume that ε is a small positive real constant, $h_0(0) = 0$, $D_y h_0(0) = 2\pi i p/q$, and that some further non-degeneracy conditions hold, see [3]. Under these assumptions system (1.5) exhibits a $p : q$-resonant HNS bifurcation near $\mu = 0$. By applying appropriate near-identity transformations and a Van der Pol transformation, the Poincaré–Takens normal form procedure yields a system with a $\mathbb{Z}_q$-symmetric and t-independent $(q-1)$-jet [11, 12]. If the vector field corresponding to the $(q-1)$-jet of the planar first component of this normal form is denoted with N_μ, then a Poincaré map of (1.2) is given by

$$P_\mu(y) = \quad _{p/q} \quad N_\mu^1(y) + O(|y|^q), \tag{1.6}$$

up to a diffeomorphism [13, 14]. Here $\quad _{p/q}$ is the rotation over $2\pi p/q$ around the origin and N_μ^1 is the time-1-map of N_μ. The dependence of N_μ on ε is not explicitly indicated, since ε is a constant. An important feature of the Poincaré–Takens normal form system is that it still exhibits dynamical properties of the original system. Moreover, by (1.6) the local q-periodic orbits of P_μ are approximately given by the local equilibria of N_μ.

We focus on the $(q-1)$-jet of the Poincaré–Takens normal form, since only this jet appears explicitly in (1.6). In the non-degenerate case the polynomial vector field N_μ can be simplified to the system $\dot{z} = \mathcal{F}_\sigma(z)$ with

$$\mathcal{F}_\sigma(z) = z(\sigma + |z|^2) + \overline{z}^{q \quad 1}, \tag{1.7}$$

Table 1. Relations between the dynamics of vector fields determined by $\mathcal{F}_\sigma$ given in (1.7) or $\mathcal{G}_{\sigma,\tau}$ given in (1.8) and corresponding Poincaré maps they approximate. The first five rows give the relations between local dynamical properties, while the latter two rows give generically expected relations between more global features.

Approximating vector field	Poincaré map
equilibrium	fixed point
q different equilibria invariant under $_{p/q}$	q-periodic orbit
(degenerate) Hopf bifurcation	(degenerate) HNS bifurcation
saddle-node bif. of q different equilibria	saddle-node bif. of q-periodic orbit
cusp bif. of q different equilibria	cusp bifurcation of q-periodic orbit
homoclinic connection	homoclinic tangle
heteroclinic connection	heteroclinic tangle

where $\sigma = \sigma_1 + i\sigma_2 \in \mathbb{C}$, by a locally diffeomorphic transformation of state space and a submersive reparametrization of the multi-parameter. In the mildly degenerate case N_μ can be simplified to the system $\dot{z} = \mathcal{G}_{\sigma,\tau}(z)$ with

$$\mathcal{G}_{\sigma,\tau}(z) = z(\sigma + \tau|z|^2 + |z|^4) + \overline{z}^{q\ \ 1}, \tag{1.8}$$

where $(\sigma, \tau) = (\sigma_1 + i\sigma_2, \tau_1 + i\tau_2) \in \mathbb{C}^2$. For details see the next section. We note that the systems $\dot{z} = \mathcal{F}_\sigma(z)$ and $\dot{z} = \mathcal{G}_{\sigma,\tau}(z)$ may not be structurally stable.

Local dynamical features of a Poincaré map only depend on a finite order jet, so all such features of (1.5), see Table 1, are determined by $\mathcal{F}_\sigma$, if the system is non-degenerate, and by $\mathcal{G}_{\sigma,\tau}$, if the system is mildly degenerate. On the other hand, more global phenomena, like heteroclinic connections, do not translate one-to-one between maps and approximating vector fields, since such dynamics also depends on higher order terms. Nevertheless, parameter values for which homoclinic or heteroclinic connections occur generically do turn into open regions corresponding to homoclinic or heteroclinic tangles, see [5, 6, 15].

Remarks.

1. By computing a Poincaré map for (1.5), utilizing the Poincaré–Takens normal form procedure, we encounter a simple approximating planar $\mathbb{Z}_q$-symmetric vector field N_μ of which the bifurcation diagram provides topological information on the dynamics of the original system.

2. We can also consider the procedure the other way around: For a given family of planar diffeomorphisms undergoing a resonant bifurcation, the normal form N_μ provides a vector field approximation. The latter point of view is useful for studying the dynamics in families of diffeomorphisms near resonance.

3. The form (1.5) also appears when periodic evolutions of autonomous systems are studied using center manifold reduction [6].

Bifurcation diagram of $\dot{z} = \mathcal{G}_{\sigma,\tau}(z)$. The bifurcation diagram of $\dot{z} = \mathcal{F}_\sigma(z)$ is already given in Fig. 2. So we proceed with brie"y demonstrating the complexity of the bifurcation diagram in the mildly degenerate case by considering an interesting 2-dimensional cross-section of the bifurcation set corresponding to $\dot{z} = \mathcal{G}_{\sigma,\tau}(z)$ for $q = 7$. More specifically, Fig. 4 displays such a section for $(\tau_1, \tau_2) = (-0.1, 0)$. The following codimension 1 bifurcation curves occur:

1. The curve *Ho* of Hopf bifurcations. Crossing this curve transversally from $\sigma_1 < 0$ to $\sigma_1 > 0$ causes the central equilibrium to loose stability.

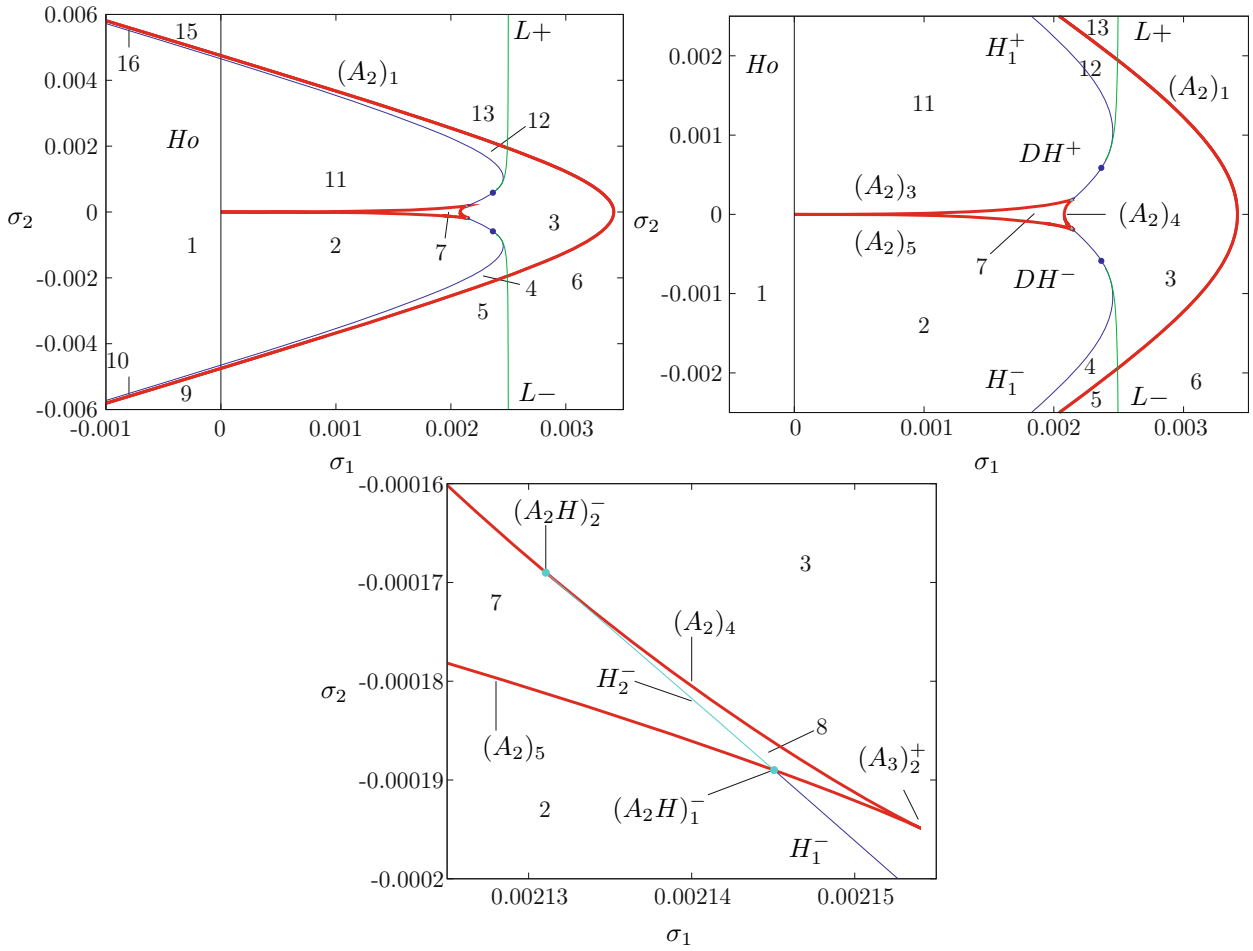

Fig. 4. Bifurcation set of the planar Poincaré–Takens normal form system $\dot{z} = \mathcal{G}_{\sigma,\tau}(z)$ given in (1.8) for $\tau = (-0.1, 0)$ and $q = 7$, with two subsequent magnifications in the (σ_1, σ_2)-parameter plane near interesting regions. See Section 1.2 for the meaning of the symbols. The curves of type A_2 are fatter to facilitate the identification of the resonance set.

2. The curves $(A_2)_k$, with $k = 1, \ldots, 5$, of saddle-node bifurcations of equilibria.

3. The curves $L^{\pm}$ of saddle-node bifurcations of limit cycles.

4. The curves $H^{\pm}_{1,2}$ of heteroclinic bifurcations of equilibria. The heteroclinic connections taking place for parameter values on the curves $H^{\pm}_1$ form heteroclinic cycles [6, Section 9.5].

Moreover, the following codimension 2 bifurcation points occur:

1. The points $A^{\pm}_3$ of cusp bifurcations of equilibria.

2. The points $DH^{\pm}$ of degenerate heteroclinic bifurcations of equilibria, where the curves $L^{\pm}$ are attached to the curves $H^{\pm}_1$.

3. The points $(A_2H)^{\pm}_{1,2}$ of degenerate heteroclinic bifurcations of equilibria. At $(A_2H)^{\pm}_1$ two curves of heteroclinic bifurcations are attached to an A_2 curve. At $(A_2H)^{\pm}_2$ the curves $H^{\pm}_2$ end on $(A_2)_4$.

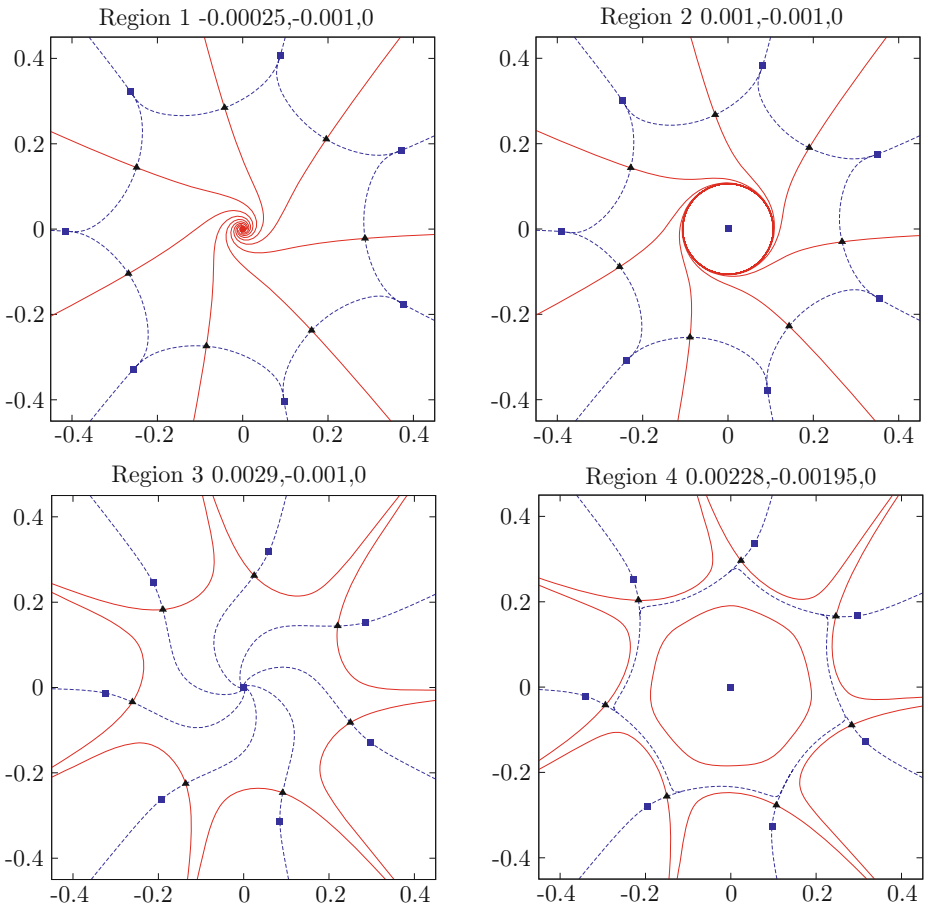

Fig. 5. Phase portraits of the system $\dot{z} = \mathcal{G}_{\sigma,\tau}(z)$. The values of σ_1, σ_2 and τ_2, as well as the corresponding region in the parameter plane (see Fig. 4), are indicated on top of each plot. From region 1 to 2 the central equilibrium undergoes the Hopf bifurcation *Ho*. In these regions there is also an unstable phase-locked invariant cycle surrounding the origin. When parameters are moved from region 2 to 3 the attracting limit cycle turns into a heteroclinic cycle at the heteroclinic bifurcation H_1^- and disappears. Between region 3 and 4 the saddle-node bifurcation L^- of limit cycles occurs. For bifurcations between neighboring regions that are not yet discussed we refer to Fig. 4.

Although the cross-section of parameter space with $(\tau_1, \tau_2) = (-0.1, 0)$ does not contain any homoclinic bifurcations, they do occur in cross-sections corresponding to other values of τ.

The above bifurcation curves induce a subdivision of the (σ_1, σ_2)-parameter plane into 16 regions. If (σ_1, σ_2)-parameter values are varied within a region, then the corresponding phase portraits remain topologically equivalent. On the other hand, if the boundary of a region is crossed transversally, then the corresponding topology changes at the crossing. We only present phase portraits for regions 1-10 (see Figs. 5, 6, and 7), since if $\tau = \overline{\tau}$ (in particular, if $(\tau_1, \tau_2) = (-0.1, 0)$), then the system $\dot{z} = \mathcal{G}_{\sigma,\tau}(z)$ is invariant under the transformation

$$\sigma \mapsto \overline{\sigma}, \qquad z \mapsto \overline{z}. \tag{1.9}$$

Remark 1. The following typographical conventions are adopted for the phase portraits in Figs. 5, 6, and 7. Attracting (repelling) periodic orbits are represented by solid (dashed) curves. Similarly, unstable (stable) manifolds of saddle equilibria are represented by solid (dashed) curves. Equilibria are also plotted differently according to their stability properties: Attractors, repellors and saddles are plotted with small disks, squares and triangles, respectively.

2. MAIN TOOLS

Here we explain the main tools, i.e., Lyapunov–Schmidt reduction and singularity theory, for showing what types of geometry of the resonance set occur in the non-degenerate and a mildly

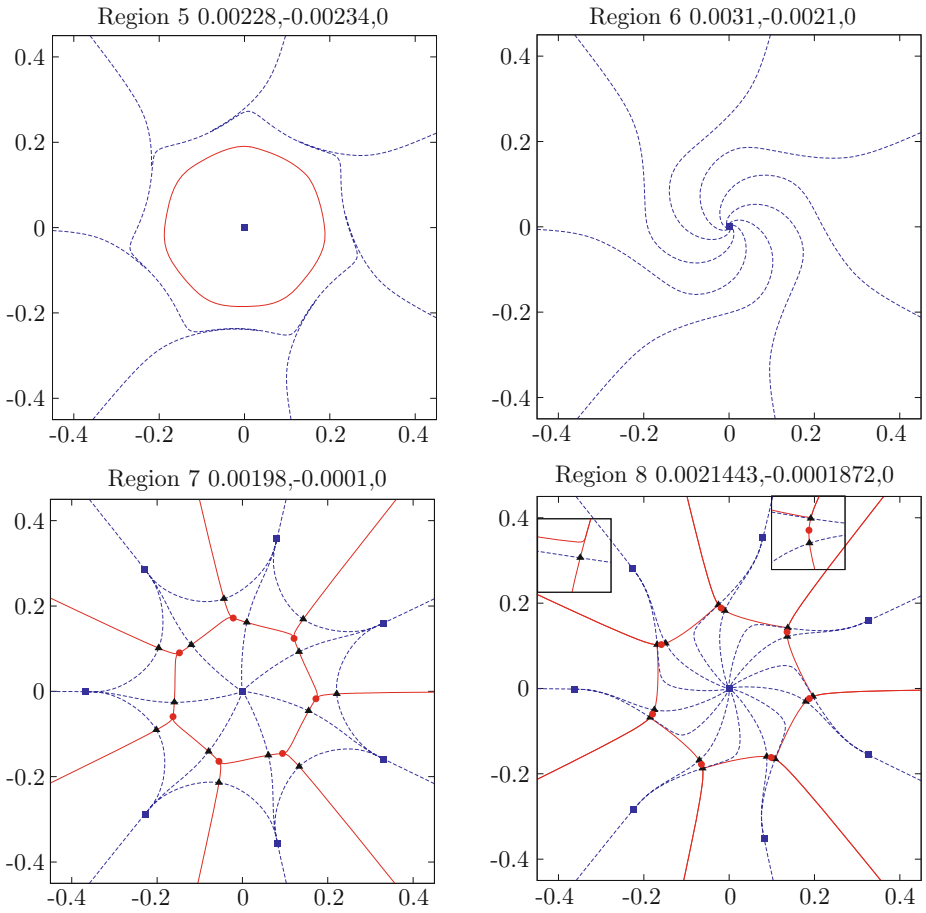

Fig. 6. Continuation of Fig. 5. For region 8, two subsequent magnifications near one of the saddles have been added in the boxes. Between regions 5 and 6 there is the saddle-node bifurcation L^- of limit cycles. Changing parameters from region 7 to regions 8 causes the "inner cycle" and "outer cycle" in region 7 to be broken up by the heteroclinic bifurcation H_2^-. For bifurcations between neighboring regions that are not yet discussed we refer to Fig. 4.

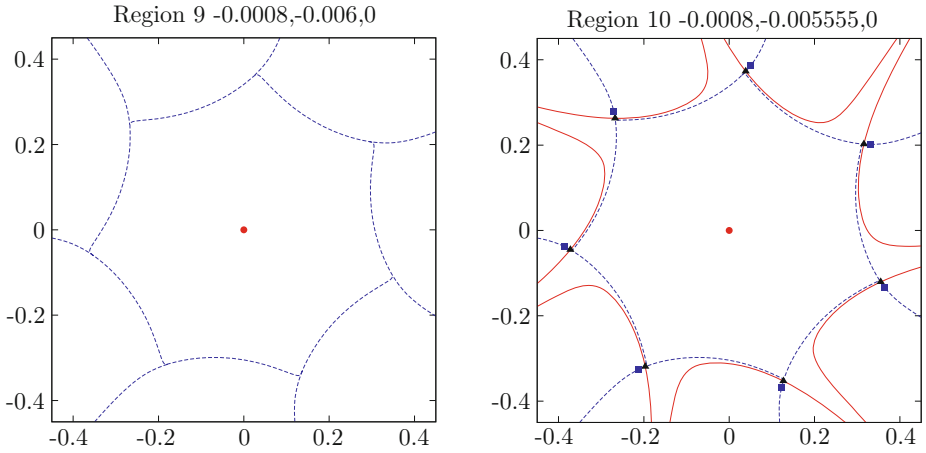

Fig. 7. Continuation of Fig. 6. Phase portraits for regions 11–16 are not included because, due to the symmetry in (1.9), up to mirroring in the x-axis they are the same as the phase portraits for regions 2, 4, 5, 8, 9 and 10, respectively. Moving parameters from region 10 to region 9 the saddle-node bifurcation $(A_2)_1$ between two sets of $\mathbb{Z}_7$-symmetric equilibria occurs. For bifurcations between neighboring regions that are not yet discussed we refer to Fig. 4.

degenerate case. Moreover, we provide the solution of the accompanying recognition problem. To this end we focus on the general setting of resonant families of diffeomorphisms.

2.1. Lyapunov–Schmidt Reduction

Our method to determine resonance sets for discrete systems proceeds as follows. Obtain parameter values for which a family of smooth diffeomorphisms $P_\mu : \mathbb{R}^m \to \mathbb{R}^m$, with $2 \leqslant m \in \mathbb{N}$ and μ near $0 \in \mathbb{R}^n$, has q-periodic orbits, i.e., solve the equation $P_\mu^q(x) = x$. Utilizing a method due to Vanderbauwhede [16], we can solve for such orbits by Lyapunov–Schmidt reduction. More precisely, a q-periodic orbit consists of q points $x_1, \ldots, x_q$, where

$$P_\mu(x_1) = x_2, \ldots, P_\mu(x_{q\ \ 1}) = x_q, P_\mu(x_q) = x_1.$$

These orbits are the zeros of the family $P_\mu : (\mathbb{R}^m)^q \to (\mathbb{R}^m)^q$ given by

$$P_\mu(x_1, \ldots, x_q) = (P_\mu(x_1) - x_2, \ldots, P_\mu(x_q) - x_1).$$

This map is $\mathbb{Z}_q$-equivariant. More specifically, if we define $\ : (\mathbb{R}^m)^q \to (\mathbb{R}^m)^q$, which generates a $\mathbb{Z}_q$-action on $(\mathbb{R}^m)^q$, as follows,

$$(x_1, \ldots, x_q) = (x_2, \ldots, x_q, x_1),$$

then

$$P_\mu = P_\mu \quad .$$

Notice that by considering P_μ the $\mathbb{Z}_q$-symmetry of q-periodic points of P_μ has become a full symmetry.

Assuming that $P_\mu(0) = 0$ and that the map $D_x P_0(0)$ has only two critical eigenvalues of the form $e^{\pm 2\pi i p/q}$ implies that the kernel of $D_y P_0(0)$, with $y = (x_1, \ldots, x_q)$, is 2-dimensional. Hence, the implicit function theorem cannot be used to solve $P_\mu(y) = 0$ near $\mu = 0$. However, Lyapunov–Schmidt reduction allows us to reduce the latter equation to finding zeros of a reduced map from $\mathbb{R}^2$ to $\mathbb{R}^2$. Identifying $\mathbb{R}^2$ with $\mathbb{C}$, we need to obtain the zeros of a reduced family $G_\mu : \mathbb{C} \to \mathbb{C}$ with $G_\mu(0) = 0$ and $D_z G_0(0) = 0$. This family also inherits the symmetry of P_μ, i.e., let $\ $ be a critical eigenvalue of $D_x P_0(0)$, then

$$G_\mu(\ \ z) = \ \ G_\mu(z).$$

As $\ $ generates an action of the group $\mathbb{Z}_q$ on $\mathbb{C}$, we have that G_μ is $\mathbb{Z}_q$-equivariant. Due to this symmetry and the property that G_0 has a singular zero at $z = 0$, $\mathbb{Z}_q$-equivariant contact-equivalence singularity theory provides a natural setting for the study of G_μ.

2.2. $\mathbb{Z}_q$-equivariant Contact-equivalence Singularity Theory

In this subsection we derive normal forms for the families G_μ by applying singularity theory. To begin with, we present a standard form for a family of planar $\mathbb{Z}_q$-equivariant smooth (non-analytic) germs, which is given by

$$G_\mu(z) = K_\mu(u, v)z + L_\mu(u, v)\overline{z}^{q\ \ 1}, \tag{2.1}$$

where $u = |z|^2, v = z^q + \overline{z}^q$ and K_μ, L_μ are uniquely defined complex-valued $\mathbb{Z}_q$-invariant map germs [1].

Contact-equivalence Contact-equivalence singularity theory approaches the study of zeros of a family by implementing coordinate changes that transform the family to a simple normal form and then solve the normal form equation. To make this precise we introduce n-parameter $\mathbb{Z}_q$-contact-equivalence transformations, which are given by a pair of the form (S_μ, Z_μ), where $S_\mu : \mathbb{C} \to \mathbb{C}\backslash\{0\}$ is a smooth map germ satisfying $S_0(z) = 1$ and $S_\mu(\ \ z) \ \ = \ \ S(z)$, with $\ \ = e^{2\pi i p/q}$, and $Z_\mu : \mathbb{C} \to \mathbb{C}$ is a $\mathbb{Z}_q$-equivariant diffeomorphism germ, with $Z_0(z) = z$. We call the two planar $\mathbb{Z}_q$-equivariant

families H_μ and G_μ $\mathbb{Z}_q$-contact-equivalent if there is a $\mathbb{Z}_q$-contact-equivalence transformation (S_μ, Z_μ), such that

$$H_\mu(z) = S_\mu(z)G_\mu(Z_\mu(z)).$$

It follows that contact-equivalences preserve the zeros of a map up to a diffeomorphism.

Recognition conditions. Now we are in the position to characterize two classes of $\mathbb{Z}_q$-equivariant families. The non-degenerate case corresponds to families of which only the linear part becomes zero for $\mu = 0$, while in the mildly degenerate case all coefficients of terms up to third order become zero for $\mu = 0$. More specifically, consider (2.1), with $K_0(0,0) = 0$, since $D_zG_0(0) = 0$ for the Lyapunov–Schmidt reduced function, and $L_0(0,0) \neq 0$, which we impose to avoid high degeneracies, then the following results hold.

1. If $D_uK_0(0,0) \neq 0$, $q \geqslant 5$ and if
$$\mu \mapsto (\mathrm{Re}(K_\mu(0,0)), \mathrm{Im}(K_\mu(0,0))) \tag{2.2}$$
is a submersion at $\mu = 0$, then G_μ is $\mathbb{Z}_q$-contact-equivalent to the normal form for the non-degenerate case given by $\mathcal{F}_{\sigma(\mu)}$ in (1.7). Here the notation $\sigma(\mu)$ indicates that besides a contact-equivalence transformation also a smooth submersive reparametrization of parameter space is needed to obtain the normal form.

2. If $D_uK_0(0,0) = 0$, $D_u^2K_0(0,0) \neq 0$, $q \geqslant 7$ and if
$$\mu \mapsto (\mathrm{Re}(K_\mu(0,0)), \mathrm{Im}(K_\mu(0,0)), \mathrm{Re}(D_uK_\mu(0,0)), \mathrm{Im}(D_uK_\mu(0,0))) \tag{2.3}$$
is a submersion at $\mu = 0$, then G_μ is $\mathbb{Z}_q$-contact-equivalent to the normal form for the mildly degenerate case given by $\mathcal{G}_{\sigma(\mu),\tau(\mu)}$ in (1.8). Here the notation $\sigma(\mu)$ and $\tau(\mu)$ indicates that again a smooth submersive reparametrization of parameter space is needed to obtain the normal form.

Remarks.

1. The latter recognition conditions on K_μ and L_μ distinguishing between the non-degenerate and mildly degenerate case can also be applied to the $\mathbb{Z}_q$-equivariant $(q-1)$-jet of the Poincaré–Takens normal form vector field of the previous section.

2. The normal forms $\mathcal{F}_\sigma$ and $\mathcal{G}_{\sigma,\tau}$ are universal unfoldings of the degenerate germs $\mathcal{F}_0$ and $\mathcal{G}_{0,0}$ respectively. This means that every $\mathbb{Z}_q$-equivariant parameter dependent deformation of $\mathcal{F}_0$ is $\mathbb{Z}_q$-contact-equivalent to $\mathcal{F}_\sigma$ up to a reparametrization of parameter space and, additionally, the number of parameters is minimal for this property to be satisfied. This minimal number of parameters is the codimension of $\mathcal{F}_0$. The same relations hold between $\mathcal{G}_{0,0}$ and $\mathcal{G}_{\sigma,\tau}$.

3. Gradual violation of degeneracy conditions, like $L_0(0,0) \neq 0$, gives rise to a familiar endless sequence of cases with ever higher codimension.

Resonance sets. Finally, we are in the position to determine the geometry of generic resonance sets. To this end we consider the corresponding boundaries, which are given by parameter values for which the number of q-periodic orbits of P_μ, or zeros of G_μ, changes. These changes occur when G_μ has a singular zero, i.e., for parameter values on the discriminant set of G_μ given by

$$\{\mu \in \mathbb{R}^n \mid \text{ there exists a } z \text{ such that } G_\mu(z) = 0 \text{ and } \det(D_zG_\mu(z)) = 0\}.$$

We observe that discriminant sets are preserved by contact-equivalences. Hence, in the non-degenerate case the boundary of the resonance set is diffeomorphic to the Cartesian product of $\mathbb{R}^{n\ 2}$ and the discriminant set of $\mathcal{F}_\sigma$. In the mildly degenerate case the boundary is diffeomorphic to the Cartesian product of $\mathbb{R}^{n\ 4}$ and the discriminant set of $\mathcal{G}_{\sigma,\tau}$.

3. CONCLUSION AND FUTURE WORK

The main aim of the current paper is presenting a novel practical procedure to detect non-degenerate and mildly degenerate Hopf–Neĭmarck–Sacker bifurcations in families of periodically forced oscillators. In particular, the mildly degenerate situation forms a next case in the general program for recognizing bifurcations, cf. [6]. We also explain how recognition conditions for HNS families determine the local geometry of the resonance set attached to the central resonant HNS bifurcation point. As an illustration, the results are applied in a leading example: A generalized Duffing–Van der Pol oscillator.

Moreover, we show that the resonance set, up to a small diffeomorphic distortion, forms only a small part of a more complicated bifurcation set, which is obtained using a Poincaré–Takens normal form vector field approximation of the family of diffeomorphisms. The 2-dimensional tomograms of parameter space investigated for this family of vector fields demonstrate a rich variety of bifurcations including (degenerate) Hopf, homoclinic, heteroclinic and Bogdanov–Takens bifurcations. A more complete study of the bifurcation set of both the mildly degenerate universal family and the corresponding vector field approximation remain future work.

An interesting extension of the current paper is formulating the recognition conditions for families of vector fields with a periodic orbit in $\mathbb{R}^k$, where $k \geqslant 3$, without assuming the reduction to the center manifold has been performed already, cf. [6].

REFERENCES

1. Broer, H., Golubitsky, M., and Vegter, G., The Geometry of Resonance Tongues: A Singularity Approach, *Nonlinearity*, 2003, vol. 16, pp. 1511–1538.
2. Broer, H., Holtman, S., and Vegter, G., Recognition of the Bifurcation Type of Resonance in Mildly Degenerate Hopf–Neĭmark–Sacker Families, *Nonlinearity*, 2008, vol. 21, pp. 2463–2482.
3. Broer, H., Holtman, S., and Vegter, G., Recognition of Resonance Type in Periodically Forced Oscillators, *Physica D*, 2010, vol. 239, pp. 1627–1636.
4. Broer, H., Holtman, S., and Vegter, G., and Vitolo, R., Geometry and Dynamics of Mildly Degenerate Hopf–Neĭmarck–Sacker Families Near Resonance, *Nonlinearity*, 2009, vol. 22, pp. 2161–2200.
5. Arnol'd, V.I., *Geometrical Methods in the Theory of Ordinary Di erential Equations*, Berlin: Springer, 1982.
6. Kuznetsov, Y., *Elements of Applied Bifurcation Theory*, *Applied Mathematical Sciences*, vol. 112, Berlin, New-York: Springer, 1995.
7. Broer, H., Naudot, V., Roussarie, R., Saleh, K., and Wagener, F., Organising Centres in the Semi-global Analysis of Dynamical Systems, *Int. J. Appl. M. Stat.*, 2007, vol. 12, no. D07, pp. 7–36.
8. Siewe, M., Kameni, F., and Tchawona, C., Resonant Oscillation and Homoclinic Bifurcation in a ^{6}-van der Pol Oscillator, *Chaos, Solitons and Fractals*, 2004, vol. 24, no. 4, pp. 841–853.
9. Duffing, G., Erzwungene schwingungen bei veränderlicher eigenfrequenz, Braunschweig: F. Vieweg u. Sohn 1918.
10. van der Pol, B. and van der Mark, J., Frequency Demultiplication, *Nature*, 1927, vol. 120, pp. 363–364.
11. Broer, H., Golubitsky, M., and Vegter, G., Geometry of Resonance Tongues, in *Singularity Theory. Proceedings of the 2005 Marseille Singularity School and Conference*, Hackensack, NJ: World Sci. Publ., 2007, pp. 327–356.
12. Broer, H., and Vegter, G., Generic Hopf–Neĭmarck–Sacker Bifurcations in Feed-forward Systems, *Nonlinearity*, 2008, vol. 21, pp. 1547–1578.
13. Takens, F., Forced Oscillations and Bifurcations, in *Applications of global analysis, I (Sympos., Utrecht State Univ., Utrecht, 1973)*, Comm. Math. Inst. Rijksuniv. Utrecht, No. 3-1974, Utrecht: Math. Inst. Rijksuniv. Utrecht, 1974, pp. 1–59.
14. Takens, F., Singularities of Vector Fields, *Publ. Math. IHES*, 1974, vol. 42, pp. 48–100.
15. Guckenheimer, J. and Holmes, P., *Nonlinear Oscillations, Dynamical Systems, and Bifurcations of Vector Fields*, New York: Springer, 1983.
16. Vanderbauwhede, A., Branching of Periodic Solutions in Time-reversible Systems, in *Geometry and Analysis in Non-linear Dynamics*, H. Broer and F. Takens, Eds., *Pitman Research Notes in Mathematics*, vol. 222, Pitman London, 1992, pp. 97–113.